Volume 7, Issue 1, 2017, 1913 - 1920 ISSN 2069-5837

Biointerface Research in Applied Chemistry

www.BiointerfaceResearch.com

Original Research Article Open Access Journal

Received: 13.01.2017 / Revised: 12.02.2017 / Accepted: 14.02.2017 / Published on-line: 15.02.2017

Inter-relation of surface tension and optical turbidity in self-assembled peptide amphiphiles

Huey Ling Tan [1, 2, *], Robin Curtis [1]

[1] School of Chemical Engineering and Analytical Sciences, The University of Manchester, Oxford Road, Manchester, M13 9PL, UK

[2] Faculty of Chemical Engineering, Universiti Teknologi MARA, 40450 Shah Alam, Selangor, Malaysia

*corresponding author e-mail address: ***hueyling@salam.uitm.edu.my, tan.hueyling@googlemail.com***

ABSTRACT

Self-associating amphiphilic peptides FEFKFEFK (EFK8-I) and FEFRFEFR (EFR8-I) with an alternating pattern of polar and non-polar side chains were studied to investigate the influence of physicochemical factors that govern aggregation pathways. Changes in aggregation mechanism were determined using a combination of turbidimetric-potentiometric titrations and interfacial tension measurements. The key parameters investigated were pH and NaCl concentration. Turbidity results showed that EFK8-I and EFR8-I displayed reversible aggregation pathway as a function of pH and NaCl concentration. The pathway was depend strongly on the pH history of the solution, but was weakly influenced by changes in salt concentration. That is, the effect of changing the peptide protonation state was greater than the effect of changing the screening length by raising the NaCl concentration. The results indicated that the pK_as of peptide side groups were shifted during titration where the titratable groups may be over-stabilised by the formation of salt bridges. These observations suggest a plausible aggregation mechanism in terms of monomers, pre-aggregates and aggregates. Formation of larger aggregates (when the solution had high initial pH) was mainly stabilised by hydrophobic interactions between smaller pre-aggregates. Equilibrium surface tension results well correlated with solution turbidities suggest that the surface-active species were pre-aggregates. These pre-aggregates were irreversibly formed, as indicated by the distinct degree of conformation formation that depended on pH history. Larger aggregates may unfold into a large number of smaller pre-aggregates at the air–water interface, leading to lower equilibrium surface tensions. This study ultimately provides a better understanding of controlling aggregation and predicting surface functional modification of self-assembled polypeptides.

Keywords: *Amphiphilic peptides, self-assembly, surface tension, turbidity, hydrophobicity, aggregation mechanism.*

1. INTRODUCTION

Synthetic self-assembling peptides are a promising class of materials that have been actively used as a model system to develop building blocks for novel self-assembled supramolecular materials for a broad-range of bioengineering and materials applications [1, 2]. Understanding the fundamental interfacial properties and molecular structures of peptides and proteins is important in designing and building functional nano- or microstructures for both life science and non-life science applications. These include biocompatible materials [3, 4], carriers in drug delivery systems [5, 6] and highly specific biochips [7] due to biocompatibility [8, 9], chemical diversity [10] and resemblance to proteins [11, 12]. *In vivo*, designer peptides are used to study the formation of insoluble macrostructures such as fibrils [13, 14] that are related to protein amyloid formation in diseases such as Alzheimer's, [15], type II diabetes [16] and Huntington's [17, 18].

There is a significant correlation between hydrophobicity and peptide functionality. Diverse studies [19, 20] have demonstrated that the hydrophobicity characteristics of a peptide influence its global structural features as well as its selectivity and activity with other biomolecules. The hydrophobic characteristics of peptides are related to surface activity. Knowledge of the interplay between interfacial properties, electrostatic interactions and conformational transitions is crucial for understanding optimal interactions and functionality of peptides [21 - 23]. Hydrophobicity and the pattern of charges in a sequence control aggregation behaviour such as the type and size of aggregates as well as the concentration at which aggregation occurs [24 – 27]. Studies [28, 29] have shown that increasing hydrophobicity increases the propensity to aggregate at low peptide concentrations, although other significant factors such as charge distribution [30, 31] and steric packing can alter aggregation behaviour [32].

Protein conformational properties such as amphiphatic structure, molecular flexibility, secondary structure and the resulting interfacial behaviour are significantly influenced by electrostatic interactions and net charge between charged amino acids. The role of electrostatic interactions in the different steps in aggregation pathways can be investigated by changing the ionic strength, which weakens electrostatic interactions through charge-screening effects. In such cases, increase in adsorption rate and surface pressure were observed with increasing ionic strength [33]. A similar effect can be probed by changing the pH, which alters the charged states of the peptide. Highest total absorbed amount and absorption rate were found when peptides has a net charge of zero. Varying pH can indirectly alter aggregation pathways by impacting upon the secondary structure propensity of the peptide. For instance, polylysine underwent conformational transformation from α-helix to β-sheet when most of the lysine residues in the sequence carried a net positive charge [34, 35]. Similarly, β-amyloid peptide was found to change from helical structures to β-sheet structures near isoelectric point [36]. FEFK [3, 37] showed a significantly slow aggregation rate when the peptide carried a net positive charge. Generally, having a net charge on the peptide is a prerequisite for fibril formation as net neutral peptides form amorphous aggregates [38, 39].

Similarly, the adsorption of proteins at interfaces is known to play a key role in structure–function relationships. Extensive

research has been carried out to investigate the interfacial properties of protein at air–water and oil–water interfaces. Only a few biophysical studies have been performed on synthetic and natural peptides to understand interfacial properties. In addition to the relatively discrete and unstable self-assembling structures, characterising the intermediates in the aggregation pathway is extremely difficult and challenging. Consequently, this study is important to provide insights into the fundamental links between self-assembly behaviours and mechanisms, highlighting the behaviour and surface activity of absorbed peptides at the air–water interface. Therefore, it is important to determine the roles of surface charge and hydrophobicity on interfacial properties. The octapeptides investigated in our work were based on four different amino acids: phenylalanine (F), glutamic acid (E), lysine (K) and arginine (R). F is a non-charged, hydrophobic amino acid. This amino acid was used to modify the overall hydrophobicity of the octapeptides. R and K are hydrophilic amino acids and have side chains that are positively charged, with pK_as of 12.4 and 10.5, respectively. The difference in the pK_a and crystal contact propensities between R and K (R is more favourable than K) provides a rational model for identifying the intermolecular forces that control self-assembly. Each of the peptides EFK8-I (FEFKFEFK) and EFR8-I (FEFRFEFR) is joined in a sequence of eight amino acids of F-E-K and F-E-R, respectively. All the hydrophobic and hydrophilic amino acids of these two oligopeptides are organised in alternating sequence. EFK8-I and EFR8-I are characterised by negative and positive charges alternating in sequence (− + − +). Studies were carried out on peptide solutions where the concentrations were below the critical gelation concentration of the peptide solutions. Turbidimetric-potentiometric titration was used to gain insights into peptide properties in bulk solution. The turbidity in the peptide solution reflected an increase in self-assembled aggregation size once aggregates were formed. The contribution of peptide hydrophobicity, electrostatics and side chain interactions to net peptide–peptide interaction was probed by changing the ionic strength and pH of the solution. Thereafter, a study to understand the mechanism of peptide self-assembly was carried out. In this work, dynamic surface tension measurement was employed to investigate the solution properties of EFK8-I at the air–water interface. Through these approaches, an aggregation mechanism was proposed. Our results highlight the importance of molecular interactions and peptide conformational stability.

2. EXPERIMENTAL SECTION

2.1. Materials and Peptide Solution Preparation. The peptides EFK8-I and EFR8-I were synthesised using standard Fmoc-based, solid-phase peptide synthesis and purified by reverse-phase high-performance liquid chromatography. The details of the experimental procedure have been reported previously [40]. Filtered (0.2 μm from VWR) solvent was used as a blank in all experiments. For turbidimetric titration measurements, 15 mL of 0.1 g/L peptide solution was prepared by dissolving the peptide in buffer solution under mild agitation with stirring. The buffer solutions were either pure deionised water (18 Ω) or solutions containing NaCl at various concentrations. These solutions were prepared by dissolving the corresponding amount of sodium chloride in deionised water, and filtered with a 0.2 μm filter before dissolution of the peptide. In addition, diluted (0.05 M) or concentrated (2 M) solutions of hydrochloric acid (HCl) or sodium hydroxide (NaOH) were used to titrate the peptide solutions.

Surface tensions were either measured as a function of peptide concentration or pH. When performing measurements as a function of peptide concentration, the solutions were prepared by dissolving the peptide in filtered (0.2 μm) deionised water (18 Ω). Very low concentrations of peptide solutions ranging from 0.01 to 1 g/L were prepared by dilution from stock solution at a concentration of 1 g/L. On the other hand, when performing measurements as a function of pH, a series of peptide solutions with pH varying from 4 to 9 was prepared at a concentration of 0.1 g/L. The pH of these peptide solutions was adjusted from pH 4 to target pH by adding small volumes of NaOH. All the measurements were performed at room temperature on the same day as the sample preparation.

2.2. Turbidimetric - Potentiometric Titration. Turbidity measurements were carried out at 490 nm wavelength using a colorimeter probe (Brinkmann, PC 950) equipped with 2 cm path length fibre optics. The transmittance (T) mode was used and the turbidity was reported as 100 − T %, in which the reading was compared to a calibrated 100% transmittance reading by using filtered (0.2 μm) solvent as a blank. In addition, a Fisher brand Hydrus 300 pH meter with a combination electrode was used to monitor the changes of solution pH. Mild agitation (100 rpm) was applied to the solution during the measurements to ensure good mixing.

In one set of experiments, turbidity measurements were carried out simultaneously with hydrogen ion titrations at room temperature using a 0.1 g/L bulk peptide solution. Trends of titration adopted were forward, reverse and multiple cycles. Forward titration refers to titration started from a low pH of 2 or 4 while reverse titration refers to backward titration from either pH 12.5 or 11, depending on the side chain pK_as of the hydrophilic amino acids in the sequence. Forward and reverse titrations were repeated in multiple cycles. Peptide titrations were carried out with small volumes of titrants (HCl or NaOH) corresponding to pH changes close to 0.1.

2.3. Peptide Aggregation as a Function of Time. Peptide aggregation of EFK8-I was also followed *in situ* as a function of time by measuring the turbidity level. The peptide solutions were prepared at an initial peptide concentration of 0.1 g/L over a pH range of 4 to 8. In some cases, the pH of the peptide solution was raised to pH 11 before reducing it to the target pH value. Otherwise the pH of the target solution was obtained by adding NaOH solution from pH 4. The turbidity was measured immediately after the pH was adjusted to the target value, after which the solution was kept under mild agitation.

2.4. Surface Tension Measurements. Axisymmetric Drop Shape Analysis-Profile (ADSA-P) was used to measure the dynamic interfacial tensions as a function of either the peptide

concentration or pH of the peptide solution. For both approaches, measurements were carried out by using an FTÅ 32 commercial pendant drop tensiometer (First Ten Angstroms) equipped with FTÅ 200 software. Deionised water was used as a solvent and was filtered with a 0.2 μm filter. Peptides were then dissolved in the filtered water using dust-free vials. In one experiment, surface tension was measured as a function of peptide concentration ranging from 0.01 to 1 g/L; these solutions were prepared by diluting a 1 g/L peptide stock solution. In our second approach, surface tension was measured as a function of pH for 0.1 g/L peptide solutions with pH varying from 4 to 9. The pH of these solutions was adjusted by HCl or NaOH. In some cases, the surface tension measurements were performed on freshly prepared peptide solutions, whereas in other instances the peptide solutions were allowed to age for 8 h before the surface tension measurements. All experiments were conducted at room temperature.

The surface tension of the pure water was determined prior to each surface tension experiment to check the quality of the filtered deionised water. Surface tension values of 72.7 ± 0.9 mN/m were obtained and agreed well with reported literature values of 72.3–72.8 mN/m [41]. To commence the measurement, a drop of peptide solution was created. The droplet images were captured every 10 s for the first 100 s and every 30 s afterwards. Surface tensions reached an asymptotic plateau value after 30 min. To maintain a high degree of comparison and correlation, the solvents were identical with those used in turbidimetry/potentiometric titration measurements. The concentrations of the peptide samples were above their critical aggregation concentration (CAC).

3. RESULTS SECTION

3.1. Peptide Aggregation versus pH. A wide pH range of 2 to 12.5 was studied to investigate the effect of different amino acids on charge states on the aggregates formation. The side chain pK_a values of the free glutamic acid (E), lysine (K), and arginine (R) were 4.25, 10.53 and 12.4, respectively. At pH 7, amino groups are expected to be protonated and carboxylic acid groups are deprotonated. The pH of the peptide solutions was reduced to below 4.25 and raised to above 10.53 (for EFK8-I) or 12.4 (for EFR8-I), so that either E or K and R were neutralised at these pH extremes.

In Figure 1 is presented the turbidity profile of the initial clear, soluble solutions of EFK8-I and EFR8-I. The turbidity level was measured by increasing the pH of the peptide solution from 2 to 12.5, after which the solution pH was gradually reduced to 2. Samples were held for ~1 min at each pH. In the forward titrations, turbidity maxima with respect to pH were observed at around pH 7. However, higher turbidity maxima were always found for both peptides at pH 4 to 5 in the reverse titrations. White visible haze/precipitation (not shown) was formed at these turbidity maxima, with a greater amount in the reverse titrations in solutions of EFK8-I and EFR8-I.

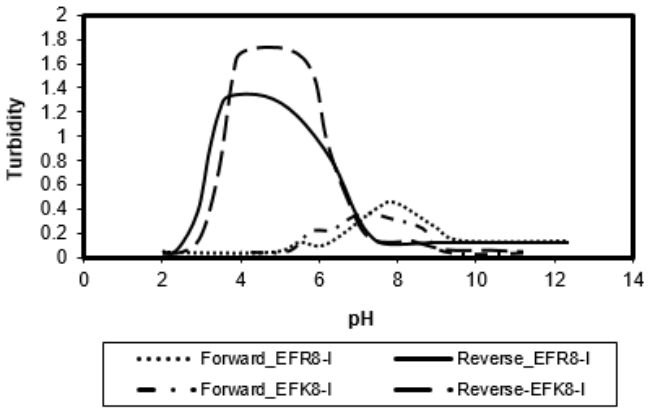

Figure 1. Turbidity profile of EFK8-I and EFR8-I as a function of pH. Measurements were started from pH 2 to either pH 11(EFK8-I) or 12.5 (EFR8-I), then back to pH 2. Higher turbidity was observed around pH 4 at the reverse segment for both the peptides.

These precipitates redissolved at pH extremes. In order to evaluate the effect of the initial solution conditions on the self-assembly behaviour, a full cycle of turbidity profiles of peptide solutions that was started in basic conditions (from pH 11 (EFK8-I) or 12.5 (EFR8-I) then lowered to 2) was also performed. The curves were reproducible upon cycling up and down in pH. Turbidity maxima were observed at pH 4 to 5 in reverse titrations and at pH 7.5 in forward titrations (results not shown), which is consistent with the results reported in Figure 1. Multiple titration cycles also yielded reproducible results for EFK8-I solution (data not shown), indicating that the aggregation behaviour was reversible. We also increased the time between successive titrant additions to ~15 min in the back titration, and found that the pH of maximum turbidity remained the same. This is consistent with previous studies [42, 43], indicating that titration curves are similar when taken over longer time scales.

The turbidity level of EFK8-I solution as a function of time was further probed *in situ* at different pH values as shown in Figure 2. Unlike the pH titration study presented earlier, in which the samples were held for ~1 min at each pH (slow titration), the pH of the freshly prepared peptide solutions was either raised (from pH 4) or lowered (from pH 11) quickly to a set of pH values between 4 and 8 (fast titration). The turbidity level was followed for 2 hours at each pH value while keeping the solutions under mild agitation. As time increased, the level of turbidity increased at different rates and reached equilibration after 40 min. Aggregate maxima were found between pH 6 and 7 in both forward and reverse fast titrations, which is close to the expected isoelectric point of the peptide. This result suggests that the aggregates formed at high turbidities were the aggregates with no net charge, in which the primary factor in the formation of larger aggregates and aggregate phase separation was reduction of charge–charge repulsions. At pH extremes, the intermediate structures formed all had charged groups accessible to the solvent, indicating an increase in net charge and minimal shielding of these charges resulting in large intermolecular repulsions. However, the turbidity maximum was much greater when the solution pH was lowered from high pH compared to that when increasing pH from 4, as shown in Figure 2. The difference in terms of the forward and

reverse turbidity maxima detected at different pH values in slow and fast titrations implies that the intermediates formed at extremes of pH have different structures depending on the memory of the solution.

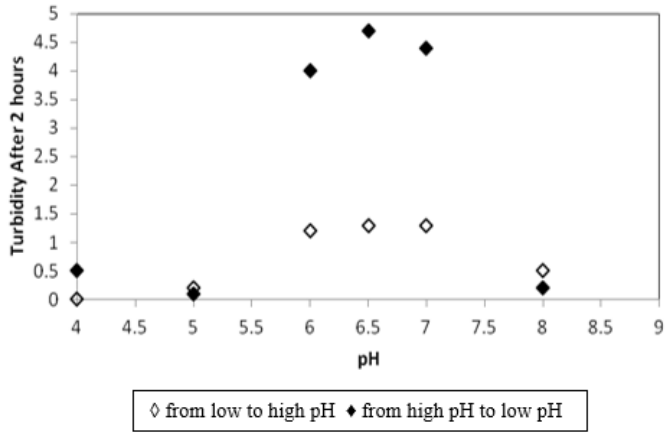

Figure 2. Final turbidity of EFK8-I solution after 2 hours of measurement. Higher maximum turbidity was observed during back titration compared to forward titration. In the present case, both forward and reverse titrations had the same pH maximum at 6.

3.2. Effects of NaCl on Aggregate Solubility. Relative aggregation rates as a function of pH and NaCl concentration were further investigated. The turbidity profiles for EFK8-I or EFR8-I solutions containing NaCl concentrations varying from 10 to 100 mM are presented in Figure 3. In these profiles, a higher maximum turbidity around pH 4 was always observed in reverse titration compared to forward titration (data not shown). In addition to the back titration, a narrowing region under the turbidity-pH curves with increasing salt concentration was observed in EFR8-I. Samples were held for ~1 min at each pH.

Increased turbidity at pH 4 observed during back titration reflects the formation of aggregates when the peptide has zero net charge. As such, at the pH of maximum turbidity, we would also expect the effect of salt to be minimal on the aggregation behaviour. This is consistent with the results observed with EFK8-I where no change in the width of the turbidity profiles was observed. A very small effect of salt (NaCl) concentration on the aggregating properties for EAK peptides was also reported [28]. This suggests that the large shift in the pH at the maximum turbidity must be a result of a large pK_a shift of the basic groups (Arginine or Lysine). It is apparent that these groups are most likely buried in aggregates that are formed as pH is gradually reduced. However, it is not clear why increasing salt concentration lowers the turbidity of the EFR8-I peptide. One hypothesis is that increasing NaCl causes the aggregates to dissociate into thinner self-assembled structures, or to undergo a transition from aggregates to monomers. Previous studies [44] indicated that charged peptides containing R can shift from β-sheet aggregates to a monomeric form in physiological-like pH (7.4) and ionic strength (130 mM NaCl). The types of short-range forces that stabilize the burial of R versus K groups are likely different. Arginine is known to form cation–pi interactions, which has been used to rationalise its propensity to be buried in protein–protein interactions formed by crystal contacts, while Lysine is generally excluded from contacts [45 – 47]. Interestingly, Arginine only has a propensity to be buried in contacts when proteins are crystallised from low versus high ionic strength solutions, a result that is consistent with our finding that increasing salt concentration weakens the forces holding aggregates together.

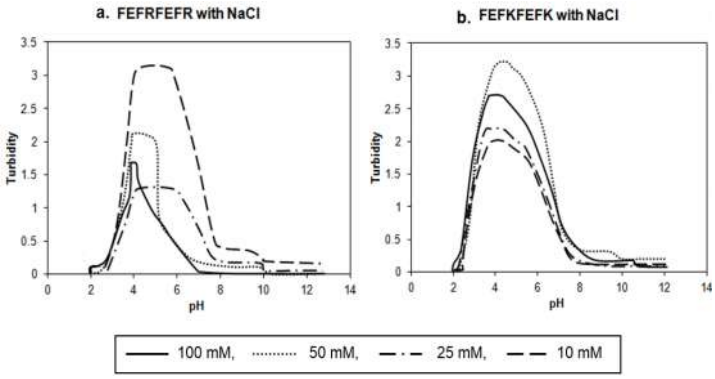

Figure 3. Turbidity profile of (a) EFR8-I and (b) EFK8-I as a function of ionic strength. These turbidity measurements were begun at peptide solutions of pH 2, up to pH 12 (EFK8-I) or 12.5 (EFR8-I) then back to pH 2. Only back-titration profiles are depicted. Forward titrations had a lower turbidity maximum at pH 6.5 (not shown). These curves were reproducible upon cycling up and down in pH (not shown).

3.3. Critical Aggregation Concentration (CAC) and Induction Time by Surface Tension. Surface tension measurements were used to study peptide aggregation in solution. A break on the plot of surface tension against peptide concentration is the CAC [26, 29, 48], whereas unchanged surface tension over an initial time period when the peptide concentration is very low is referred to as induction time. An analogy to CAC has been drawn to the critical micelle concentration (CMC) for amphiphilic molecules such as surfactants. By analogy, an amphiphilic peptide may lead to the formation of peptide self-assembled nanostructures by exhibit similar concentration-dependent behavior [30].

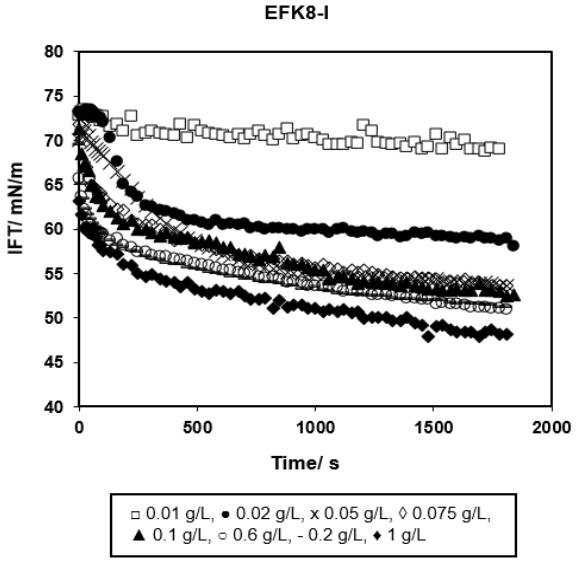

Figure 4. Dynamic surface tension profiles of EFK8-I solutions. Peptide concentrations ranged from 0.01 to 1 g/L.

Here, we performed similar dynamic surface tension profiles to probe further the aggregation behaviour of EFK8-I and EFR8-I. Figure 4 shows representative dynamic surface tension as a function of time for peptide solution concentrations varying from 0.01 to 1 g/L. At higher peptide concentrations (> 0.1 g/L), surface tension reduced significantly from 0 to 200 seconds, before gradually approached an equilibrium value. For peptide concentrations below 0.1 g/L, surface tension significantly decreased with time only after a certain time period referred to as the induction time. Here, the induction time corresponded to the reduction of 5% of surface tension value from that at time = 0

[30]. The results were plotted against peptide concentration as depicted in Figure 5. As peptide concentration increased, the induction time decreased and eventually went to zero at a peptide concentration of approximately 0.1 g/L for both EFK8-I and EFR8-I (see discussion).

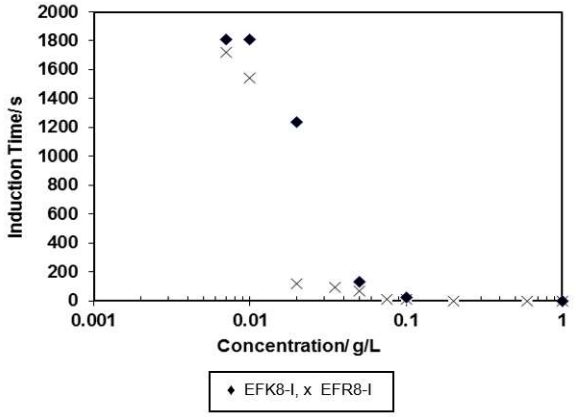

Figure 5. Induction time with solutions of EFK8-I and EFR8-I. Concentrations for both peptide solutions were varied from 0.01 to 1 g/L.

The 'extrapolation' method was employed to determine the equilibrium surface tension values [48]. Linear extrapolation of $1/t^{0.5}$ to the y axis was employed to estimate the equilibrium surface tension values. A diffusion-controlled surface adsorption mechanism was assumed in this case [49]. Linear fitting of a straight line for values of $1/t^{0.5} < 0.05$, with intercept at the y axis ($t = \infty$) is estimated to determine the equilibrium surface tension values. The value is plotted against the concentration of EFK8-I and EFR8-I as illustrated in Figure 6. Our results show that EFK8-I and EFR8-I had a CAC of 0.1 g/L.

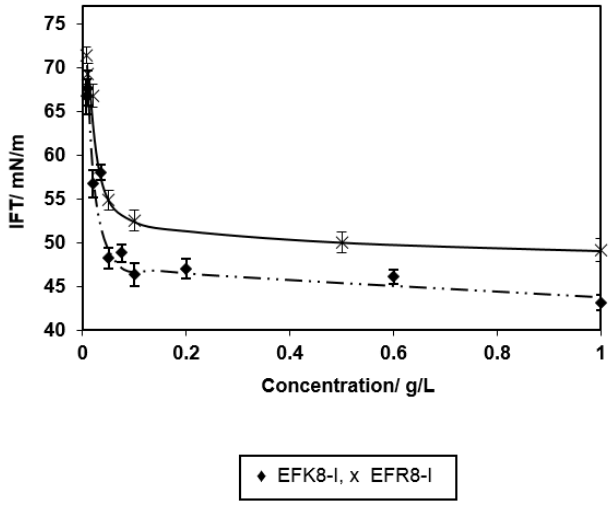

Figure 6. Relationship between quasi-equilibrium surface tension and concentration of EFK8-I, EFR8-I and EAK8-I in water solution. When the concentration increased, the surface tension dropped dramatically to a minimum value at 0.1 g/L, and then reached a plateau.

The data followed similar behaviour to micelle formation by surfactants, in which there was an initial decrease in equilibrium surface tension, followed by a region where the surface tension remained relatively constant with respect to peptide concentration. The similarity to micelle behaviour has already been observed in a series of studies on EAK peptides [15, 16, 50]. For surfactant solutions, the transition between the two regimes occurs at the CMC. Below the CMC, when increasing surfactant concentration, the surface tension decreases due to increased adsorption of surfactant. The surface tension remains constant above the CMC because increasing surfactant concentration only leads to more micelles while the surfactant monomer chemical potential remains constant. A similar analogy can be drawn to peptides, suggesting that surface-active species begin to aggregate with each other at the critical peptide concentration. Others [51] have found a connection between stages of molecular association and aggregation timescale by using nanotube-forming hexa-peri-hexabenzocoronene (hbc) molecules in a coarse-grain simulation study. According to the work, there are two aggregation stages, namely pre-aggregation and aggregation. During pre-aggregation, peptide monomers rapidly coalesce with one another to form small aggregates in the first stage. Formation of larger aggregates occurs in the second stage and takes longer time. Most self-assembly process is completed in the first two stages while the post-aggregation is mainly controlled by molecular self-organisation within the peptide aggregates.

Miller [52] explained the induction time in terms of the competition between two different adsorbed states of β-lactoglobulin at low protein concentrations that had different molecular areas. The induction time was associated with a slow rate of transfer between the two states, in which the difference in the adsorbed states could correspond to a conformational rearrangement of the protein. Thus, another possibility is that the induction time is related to a conformational rearrangement of the peptide at the interface. At the critical concentration, the surface-active species could be formed in solution, in which case the surface tension would decrease immediately due to diffusion of the species. The similarity between the critical concentrations would imply that these species can then aggregate into larger structures.

3.4. Discussion: Peptide Self-Association and Adsorption Behaviour. In order to further establish the link between aggregates and surface tension, results of equilibrium surface tensions of EFK8-I were compared with the turbidity study via quick titrations. Figure 7 shows a plot of the estimated equilibrium surface tension for 0.1 g/L EFK8-I solutions from pH 4 to 9.

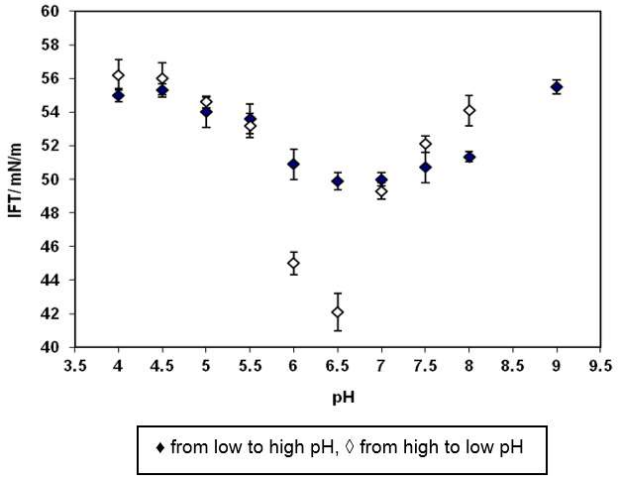

Figure 7. Relation of surface tension of EFK8-I at quasi-equilibrium with pH ranges from pH 4 to 9. The pH of the peptide solutions was either raised from low pH of 4 or reduced from 11 to a series of target pH values before the dynamic surface tension data were taken.

The peptide solutions were either raised quickly from pH 4 or reduced quickly from pH 11 to a range of target pH values. Solutions in which the pH was raised from pH 4 display an inward curve which has a minimum of 49.9 ± 0.5 mN/m at pH 6.5. Peptide solutions that were prepared by reducing the pH from 11 also display an inward curve but have a lower minimum value of

42.1 ± 0.9 mN/m at the same pH. Our results indicate that at pH 6.5, the amount of aggregates is at a maximum whereas at pH lower or higher than 6.5, there is a lower number of aggregates in solution.

Partial insight into factors controlling the surface tension can be gained from considering the limit for dilute peptide solutions, where surface tension is given by [53]:

$$\pi = \gamma_0 - \gamma \approx \Gamma RT$$

where π is the surface pressure, γ_0 and γ are the surface tension for the clean air-water interface and surface tension with surface-active species respectively, Γ is the surface excess concentration of the peptide, R is the ideal gas constant and T is the absolute temperature. According to Biswas et al. [54], the molecular adsorption process at the interface involves three steps: diffusion, transfer and rearrangement. Diffusion step involves molecular diffusion from the bulk to the sub-interface and subsequent molecular transfer to the interface. Molecular rearrangement at the interface will take place in the last step. Here, given the strong correlation between turbidity and surface tension, an increase in bulk aggregation corresponds with an increase in the number of aggregates adsorbed to the surface, resulting in a decrease in equilibrium surface tension. Reproducible higher turbidity with lower surface tension between pH 6 and 7 suggests that these aggregates may dissociate into hydrophobic pre-aggregates upon a change in solution pH and cause aggregates to grow dramatically [55, 56].

In this regard, one can argue that either the large aggregates or the smaller pre-aggregates can be adsorbed at the air–water interface. However, it is unlikely that the large aggregates are more hydrophobic as the hydrophobic groups will be hidden within the aggregates, as the formation of large aggregates is driven by hydrophobic interactions in a process that is similar to the aggregation mechanism of globular protein formation [57, 58]. Monomers, on the other hand, are unlikely to be the surface-active species, in which the exposed charged groups on the monomer have repulsive image forces with the interface. As large aggregates approach the interface, they may unfold into pre-aggregates due to weakening of hydrophobic interactions within the aggregates [59, 60]. These pre-aggregates will then rearrange themselves before they are adsorbed at the air–water interface, where the propensity of pre-aggregates to adsorb to the interface is controlled by surface hydrophobicity [61, 62]. Therefore, it is most likely that pre-aggregates are the species that govern surface activity. These hydrophobic pre-aggregates cannot inter-convert between each other as indicated by the irreversible formation (distinct association level) at pH 6.5 that depends on pH history. Thus, most probably intramolecular rearrangements of pre-aggregates cannot happen, but rearrangements can occur during dissociation of aggregates into pre-aggregates at the interface. In general, the diffusion stage is considered as the rate-determining stage since pre-aggregates diffuse faster than the larger ones, they are expected to accumulate at the interface. Consequently, surface tension may primarily reflect the behaviours of the small aggregates rather than the large ones in self-assembling peptide systems [63]. Consequently, one explanation for the correlation between surface activity and turbidity is that the enhancement of surface activity is attributed to the dissociation of large aggregates into smaller pre-aggregates, which results in an increased surface hydrophobicity that is implied by a lower surface tension.

Note that this picture is more consistent with the CMC concept, where the large aggregates are the equivalent of a micelle, and break up when diffusing to the interface as they are held together by hydrophobic interactions. This explains why the surface tension remains constant above the CAC, because the larger aggregates act as a reservoir for the generation of surface-active pre-aggregates. If it is the electrostatic interactions that hold the aggregates together, then it is unlikely that they would break apart, but this scenario is not supported by the ionic strength dependence of the turbidity behaviour.

Lower equilibrium surface tension values obtained at pH 6.5 when the peptide solutions were reduced from initially high pH compared to those where pH was raised from a low value indicate that peptide pre-aggregates are more hydrophobic when the solution environment is in an alkaline condition, in which aggregate behaviour depends upon the method of changing pH direction. EFK8-I molecules which were in alkaline solution may initially have formed a different aggregate structure in solutions at pH 6.5. These pre-aggregates are more hydrophobic in character and provide a stickier surface that can enhance aggregation. The aggregates formed may also have different polarity depending on the direction of the pH change, which in turn dictates the change in charge distribution and resulting charge–charge interactions of the aggregates at pH 6.5 (forward versus back titration). Studies have shown that the creation of such aggregates typically involves changes in the secondary structures [61, 64] that in turn depend greatly on the internal structures of the aggregates [62], while others [16] have shown that aggregate conformational changes of EAK16-IV may occur at different pH values by performing dynamic surface tension profiles to follow the conformational change of EAK16-IV aggregates near neutral pH. The behaviour of the more hydrophobic aggregates was reflected by the lower surface tension, compared to the other pH values, a finding that is consistent with our results.

4. CONCLUSIONS

This report describes the study of EFK8-I and EFR8-I aggregation as a function of pH and NaCl concentration. Peptide aggregation was highly dependent on pH and the pH history of the solution. Our results showed that the effect of changing the protonation state of the peptide on aggregation was greater than the effect of changing the screening length by raising the salt concentration. The difference in pH at maximum turbidity for slow versus quick back titration signified that the aggregation pathway was also important. Varying ionic strength did not result in changes in conformational stability of EFK8-I as its net charge was zero around pH 7. Therefore, formation of larger aggregates was probably due to no net charge between pre-aggregates. The formation of pre-aggregates occurred irreversibly from monomers, a result which was necessary to explain differences in turbidity and surface tension arising from the pH history of the solution. Furthermore, equilibrium surface tension correlated well with solution turbidity, which can be explained by assuming that the surface-active species were pre-aggregates. These pre-aggregates

formed regardless of the hydrophobicity of the peptide. Higher turbidities corresponded to the formation of larger aggregates which, in turn, dissociated to a larger number of pre-aggregates at the surface leading to lower equilibrium surface tensions. Formation of aggregates from pre-aggregates was aligned with the hydrophobicity of the peptide. The results suggest that the growth mechanism may control and predict surface functional modification of self-assembled polypeptides in creating novel functional smart biomaterials.

5. REFERENCES

[1] Zhang S. G., Altman M., Peptide self-assembly in functional polymer science and engineering, *Reactive and Functional Polymers*, 41, 91–102, **1999.**

[2] Zhang S., Buschow K. H. J., Cahn R. W., Hemings M. C., Ilschner B., Kramer E. J., Mahajan S., (Eds.) Encyclopedia of Materials: Science and Technology, Elsevier, Oxford, p. 5822, **2001.**

[3] Caplan M. R., Moore P. N., Zhang S. G., Kamm R. D., Lauffenburger D. A., Self assembly of a β-sheet protein governed by relief of electrostatic repulsion relative to van der Waals attraction, *Biomacromolecules*, 1, 627–631, **2000.**

[4] Santoso S., Zhang S., Nalwa H. S., (Eds.) Encyclopedia of Nanoscience and Nanotechnology, American Scientific Publishers, Stevenson Ranch, CA, **2003.**

[5] De Santis E., Ryadnov M. G., Peptide self-assembly for nanomaterials: the old new kid on the block, *Chemical Society Reviews*, 44, 8288–8300, **2015.**

[6] Frederix P. W. J. M., Scott G. G., Abul-Haija Y. M., Kalafatovic D., Pappas C. G., Javid N., Hunt N. T., Ulijn R. V., Tuttle T., Exploring the sequence space for (tri-) peptide self-assembly to design and discover new hydrogels, *Nature Chemistry*, 7, 30–37, **2015.**

[7] Tan H. L., Molecules and the art of self-assembly, *The Chemical Engineer*, 849, 48–51, **2012.**

[8] Zhang S., Emerging biological materials through molecular self-assembly, *Biotechnology Advances*, 20, 321–329, **2002.**

[9] Santoso S. S., Vauthey S., Zhang S., Structures, function and applications of amphiphilic peptides, *Current Opinion in Colloid and Interface Science* 7, 262–266, **2002.**

[10] Zhang S., Marini D. M., Hwang W., Santoso S., Design of nanostructured biological materials through self-assembly of peptides and proteins, *Current Opinion in Chemical Biology*, 6, 865–871, **2002.**

[11] Mandal D., Shirazi A. N., Parang K., Self-assembly of peptides to nanostructures, Organic & Biomolecular Chemistry 12:3544–3561, **2014.**

[12] Shamsudeen H, Tan HL (2015) Self-assembly of peptide amphiphiles: molecularly engineered bionanomaterials, *Advanced Materials Research*, 1113, 586–593.

[13] Wen Y., Roudebush S. L., Buckholtz G. A., Goehring T. R., Giannoukakis N., Gawalt E. S., Meng W. S., Coassembly of amphiphilic peptide EAK16-II with histidinylated analogues and implications for functionalization of β-sheet fibrils in vivo. *Biomaterials*, 35(19), 5196–5205, **2014.**

[14] Chen C., Liu Y. L., Zhang J., Zhang M. Z., Zheng J., Teng Y., Liang G. Z., A quantitative sequence-aggregation relationship predictor applied as identification of self-assembled hexapeptides, *Chemometrics and Intelligent Laboratory Systems*, 145, 7–16, **2015.**

[15] Zanuy D., Haspel N., Tsai H. H., Side chain interactions determine the amyloid organization: a single layer β-sheet molecular structure of the calcitonin peptide segment 15-19. *Physical Biology*, 1, 89–99, **2004.**

[16] Hong Y. S., Legge R. L., Zhang S., Effect of amino acid sequence and pH on nanofiber formation of self-assembling peptides EAK16-II and EAK16-IV, *Biomacromolecules*, 4, 5, 1433–1442, **2003.**

[17] Wang J., Cao Y. P., Li Q., Liu L., Dong M. D., Size effect of graphene oxide on modulating amyloid peptide assembly. *Chemistry – A European Journal*, 21, 27, 9632–9637, **2015.**

[18] Zhu D. H., Bungart B. L., Yang X. G., Zhumadiloz Z., Lee J. C. M., Askarova S., Role of membrane biophysics in Alzheimer's related cell pathways, *Frontiers in Neuroscience* 9, 186, **2015.**

[19] Li Y., Rosal R. V., Brandt-Rauf P. W., Fine R. L., Correlation between hydrophobic properties and efficiency of carrier-mediated membrane transduction and apoptosis of a p53 C-terminal peptide, *Biochemical and Biophysical Research Communications*, 298, 3, 439–449, **2002.**

[20] Dathe M., Wieprecht T., Structural features of helical antimicrobial peptides: their potential to modulate activity on model membranes and biological cells, *Biochimica et Biophysica Acta*, 1462, 71–87, **1999.**

[21] Alvares D. S., Fanani M. L., Neto J. R., Wilke N., The interfacial properties of peptide Polybia-MP1 and its interaction with DPPC are modulated by lateral electrostatic attractions, *Biochimica et Biophysica Acta*, 1858, 393–402, **2016.**

[22] Zhou P, Deng L, Wang Y, Lu JR, Xu H, Different nanostructures caused by competition of intra- and inter-β-sheet interactions in hierarchical self-assembly of short peptides, *Journal of Colloid and Interface Science*, 464, 219–228, **2016.**

[23] Mu Y., Yu M., Effects of hydrophobic interaction strength on the self-assembled structures of model peptides, *Soft Matter* 10, 27, 4956–4965, **2014.**

[24] Cui H., Cheetham A. G., Pashuck E. T., Stupp S. I., Amino acid sequence in constitutionally isomeric tetrapeptide amphiphiles dictates architecture of one-dimensional nanostructures. *Journal of the American Chemical Society*, 136, 12461–12468, **2014.**

[25] Hwang W., Marini D. M., Kamm R. D., Zhang S., Supramolecular structure of helical ribbons self-assembled from a β-sheet peptide, *Journal of Chemical Physics*, 118, 1, 389–397, **2003.**

[26] Zhang S. G., Holmes T., Lockshin C., Rich A., Spontaneous assembly of a self-complementary oligopeptide to form a stable macroscopic membrane, *Proceedings of the National Academy of Sciences of the United States of America (Chemistry)*, 90, 3334–3338, **1993.**

[27] Tekin E. D., Molecular dynamics simulations of self-assembled peptide amphiphile based cylindrical nanofibers, *RSC Advances*, 5, 82, 66582–66590, **2015.**

[28] Desii A., Chiellini F., Duce C., Ghezzi, Monti S., Tine M. R., Solaro R., Influence of structural features on the self-assembly of short ionic oligopeptides. *Journal of Polymer Science: Part A: Polymer Chemistry*, 48, 889–897, **2010.**

[29] Zou D., Tie Z., Lu C., Qin M., Lu X., Wang M., Wang W., Chen P., Effects of hydrophobicity and anions on self-assembly of the peptide EMK16-II, *Biopolymers*, 93, 4, 318–329, **2009.**

[30] Hong Y. S., Pritzker M. D., Legge R. L., Effect of NaCl and peptide concentration on the self-assembly of an ionic-complementary peptide EAK16-II, *Colloids and Surfaces B: Biointerfaces*, 46, 152–161, **2005.**

[31] Jun S., Hong Y., Imamura H., Self-assembly of the ionic peptide EAK16: the effect of charge distribution on self-assembly, *Biophysical Journal*, 87, 1249–1259, **2004.**

[32] Bowerman C. J., Ryan D. M., Nissan D. A., Nilsson B. L., Effects of hydrophobicity and anions on self-assembly of the peptide EMK16-II, *Molecular BioSystems*, 5, 1058–1069, **2009.**

[33] Mahmoudi N., Axelos A. A. V., Riaublanc A., Interfacial properties of fractal and spherical whey protein aggregates, *Soft Matter*, 7, 17, 7643–7654, **2011.**

[34] Applequist J., Doty P., Stahmann M., (Eds.) *Polyamino Acid, Polypeptides and Proteins*, University of Wisconsin, Madison, WI, p. 161, **1965.**

[35] Greenfield N., Fasman G. D., Computed circular dichroism spectra for the evaluation of protein conformation. Biochemistry 8, 4108–4116, **1969.**

[36] Barrow C. J., Zagorski M. G., Solution structures of beta peptide and its constituent fragments: relation to amyloid deposition, *Science*, 253, 179–192, **1991.**

[37] Marini D. M., Hwang W., Lauffenburger D. A., Zhang S., Kamm R. D., Left-handed helical ribbon intermediates in the self-assembly of a β-sheet peptide, *Nano Letters*, 2, 4, 295–299, **2002.**

[38] Aggeli A., Bell M., Carrick L. M., Fishwick C. W. G., Harding R., Mawer P. J., Radford S. E., Strong A. E., Boden N., pH as a trigger of peptide β-sheet self-assembly and reversible switching between nematic

and isotropic phases, *Journal of the American Chemical Society*, 125, 9619–9628, **2003.**

[39] de la Paz M. L., Goldie K., Zurdo J., Lacroix E., Dobson C. M., Hoenger A., Serrano L., De novo designed peptide-based amyloid fibrils, *Proceedings of the National Academy of Sciences of the United States of America*, 99, 25, 16052–16057, **2002.**

[40] King P. J. S., Lizio M. G., Booth A., Collins R. F., Gough J. E., Miller A. F., Webb S. J., A modular self-assembly approach to functionalised β-sheet peptide hydrogel biomaterials, *Soft Matter*, 12, 1915–1923, **2016.**

[41] Davies R. P. W., Beevers A. A., Boden N., Carrick L. M., Fishwick C. W. G., McLeish T. C. B., Nyrkova I., Semenov A. N., Self-assembling β-sheet tape forming peptides, *Supramolecular Chemistry*, 18, 5, 435–443, **2006.**

[42] Brummitt R. K., Nesta D. P., Chang L., Kroetsch A. M., Roberts C. J., Nonnative aggregation of an IgG1 antibody in acidic conditions, part 2: nucleation and growth kinetics with competing growth mechanism, *Journal of Pharmaceutical Sciences*, 100, 2104–2119, **2011.**

[43] Kroetsch A. M., Sahin E., Wang H. Y., Roberts C. J., Phase behaviour of amyloid polymers of alpha-chymotrypsinogen, *Journal of Pharmaceutical Sciences*, 101, 3651–3660, **2012.**

[44] Carrick L. M., Aggeli A., Boden N., Fisher J., Ingham E., Waigh T. A., Effect of ionic strength on the self-assembly, morphology and gelation of pH responsive β-sheet tape-forming peptides, *Tetrahedron*, 63, 31, 7457–7467, **2007.**

[45] Anstrom D. M., Colip L., Moshofsky B., Hatcher E., Remington S. J., Systematic replacement of lysine with glutamine and alanine in Escherichia coli malate synthase G: effect on crystallization, *Acta Crystallographica Section F: Structural Biology and Crystallization Communications*, F61, 1069–1074, **2005.**

[46] Dale G. E., Oefner C., D'Arcy A., The protein as a variable in protein crystallization, *Journal of Structural Biology*, 142, 88–97, **2003**

[47] Iyer G. H., Dasgupta S., Bell J. A., Ionic strength and intermolecular contacts in protein crystals, *Journal of Crystal Growth*, 217, 4, 429–440, **2000.**

[48] Fung S. Y., Keyes C., Duhamel J., Chen P., Concentration effect on the aggregation of a self assembling oligopeptide, *Biophysical Journal*, 85, 537–548, **2003.**

[49] Cabrerizo-Vilchez M. A., Policova M. A. Z., Kwok D. Y., Chen P., Neumann A. W., The temperature dependence of the interfacial tension of aqueous human albumin solution/decane, *Colloids and Surfaces B: Biointerfaces*, 5, 1–9, **1995.**

[50] Silvestri A., Fu Lu M. Y., Johnson H., Kinetics and mechanisms of peptide aggregation: aggregation of a cholecystokinin analogue, *Journal of Pharmaceutical Sciences*, 82, 689–693, **1993.**

[51] Srinivas G., Klein M. L., Molecular dynamics simulations of self-assembly and nanotube formation by amphiphilic molecules in aqueous solutions: a coarse-grain approach, *Nanotechnology*, 18, 20, 205703-205712, **2007.**

[52] Miller R. E., Aksenenko V., Fainerman V. B., Pison U., Kinetics of adsorption of globular proteins at liquid/fluid interfaces, *Colloids Surfaces A: Physiochemical and Engineering Aspects*, 183–185, 381–390, **2001.**

[53] Shaw D. J., *Introduction to Colloid and Surface Chemistry*, 4th Edition, Butterworth-Heinemann Ltd, Oxford; Boston

[54] Biswas M. E., Chatzis I., Ioannidis M. A., Chen P., Modeling of adsorption dynamics at air-liquid interfaces using statistical rate theory (SRT), *Journal of Colloid and Interface Science*, 286, 14–27, **2005.**

[55] Kroetsch A. M., Sahin E., Wang H. Y., Krizman S., Roberts C. J., Relating particle formation to salt- and pH-dependent phase separation of non-native aggregates of alpha-chymotrypsinogen A, *Journal of Pharmaceutical Sciences*, 101, 10, 3651–3660, **2012.**

[56] Sahin E., Weiss W. F., Kroetsch A. M., King K. R., Kessler R. K., Das T. K., Aggregation and pH-temperature phase behaviour for aggregates of an Igg2 antibody, *Journal of Pharmaceutical Sciences*, 101, 1678–1687, **2012.**

[57] Banks D. D., Latypov R. F., Ketchem R. R., Woodard J., Scavezza J. L., Siska C. C., Native-state solubility and transfer free energy as predictive tools for selecting excipients to include in protein formulation development studies, *Journal of Pharmaceutical Sciences*, 101, 8, 2720–2732, **2012.**

[58] Roberts C. J., Non-native protein aggregation kinetic, *Biotechnology and Bioengineering*, 98, 5, 927–938, **2007.**

[59] Bee J. S., Chiu D., Sawicki S., Stevenson J. L., Chatterjee K., Freund E., Monoclonal antibody interactions with micro- and nanoparticles: adsorption, aggregation, and accelerated states studies, *Journal of Pharmaceutical Sciences*, 98, 9, 3218–3238, **2009.**

[60] Bee J. S., Schwartz D. K., Trabelsi S., Freund E., Stevenson J. L., Carpenter J. F., Production of particles of therapeutic proteins at the air–water interface during compression/dilation cycles, *Soft Matter*, 8, 40, 10329–10335, **2012.**

[61] Wu H., Kroe-Barett R., Singh S., Robinson A. S., Roberts C. J., Competing aggregation pathways for monoclonal antibodies, *FEBS Letters*, 588, 6, 936–941, **2014.**

[62] Amin S., Barnett G. V., Pathak J. A., Roberts C. J., Sarangapani P. S., Protein aggregation, particle formation, characterisation & rheology, *Current Opinion in Colloid & Interface Science*, 19, 438–449, **2014.**

[63] Fung S. Y., Yang H., Chen P., Sequence effect of self-assembling peptides on the complexation and in vitro delivery of the hydrophobic anticancer drug ellipticine, *PLoS ONE*, 3, 4, e1956, **2008.**

[64] Latypov R. F., Hogan S., Lau H., Gadgil H., Liu D., Elucidation of acid-induced unfolding and aggregation of human immunoglobulin Igg1 and Igg2 FC, *Journal of Biological Chemistry*, 287, 2, 1381–1396, **2011.**